OXFORD

The pattern of cortical thickness underlying disruptive behaviors in Alzheimer's disease

Raymond M. Xiong[1], Teng Xie[2], Haifeng Zhang[2], Tao Li[2], Gaolang Gong[3,4,5], Xin Yu[2] and Yong He[3,4,5,*]

[1]Experimental High School Attached to Beijing Normal University, Beijing 100032, China
[2]Dementia Care & Research Center, Peking University Institute of Mental Health & National Clinical Research Center for Mental Disorders, Beijing 100191, China
[3]State Key Laboratory of Cognitive Neuroscience and Learning, Beijing 100875, China
[4]Beijing Key Laboratory of Brain Imaging and Connectomics, Beijing Normal University, Beijing 100875, China
[5]IDG/McGovern Institute for Brain Research, Beijing Normal University, Beijing 100875, China
*Correspondence: Yong He, yong.he@bnu.edu.cn

Abstract

Background Disruptive behaviors, including agitation, disinhibition, irritability, and aberrant motor behaviors, are commonly observed in patients with Alzheimer's disease (AD). However, the neuroanatomical basis of these disruptive behaviors is not fully understood.

Objective To confirm the differences in cortical thickness and surface area between AD patients and healthy controls and to further investigate the features of cortical thickness and surface area associated with disruptive behaviors in patients with AD.

Methods One hundred seventy-four participants (125 AD patients and 49 healthy controls) were recruited from memory clinics at the Peking University Institute of Sixth Hospital. Disruptive behaviors, including agitation/aggression, disinhibition, irritability/lability, and aberrant motor activity subdomain scores, were evaluated using the Neuropsychiatry Inventory. Both whole-brain vertex-based and region-of-interest-based cortical thickness and surface area analyses were automatically conducted with the CIVET pipeline based on structural magnetic resonance images. Both group-based statistical comparisons and brain-behavior association analyses were performed using general linear models, with age, sex, and education level as covariables.

Results Compared with healthy controls, the AD patients exhibited widespread reduced cortical thickness, with the most significant thinning located in the medial and lateral temporal and parietal cortex, and smaller surface areas in the left fusiform and left inferior temporal gyrus. High total scores of disruptive behaviors were significantly associated with cortical thinning in several regions that are involved in sensorimotor processing, language, and expression functions. The total score of disruptive behaviors did not show significant associations with surface areas.

Conclusion We highlight that disruptive behaviors in patients with AD are selectively associated with cortical thickness abnormalities in sensory, motor, and language regions, which provides insights into neuroanatomical substrates underlying disruptive behaviors. These findings could lead to sensory, motor, and communication interventions for alleviating disruptive behaviors in patients with AD.

Keywords: Disruptive behaviors; Alzheimer's disease; cortical thickness; surface area; magnetic resonance imaging (MRI); CIVET algorithm

Introduction

As the elderly population increases, the number of people suffering from Alzheimer's disease (AD) has increased dramatically. Statistics have indicated that a new dementia patient is diagnosed every 3 seconds, of which 60–80% are AD patients (Alzheimer's Disease International, 2015, 2021). Neuropsychiatric symptoms in AD patients, especially disruptive behavioral problems, can increase caregiver stress, disrupt daily life, and potentially endanger patients, family members, and caregivers. However, the neural mechanisms underlying disruptive behaviors have yet to be elucidated.

In clinical practice, agitation, disinhibition, irritability, and aberrant motor behaviors are considered disruptive. Agitation includes excessive motor activity, physical aggression, and verbal aggression. Disinhibition refers to inappropriate and impulsive behaviors, attention deficit behaviors, weakened emotional regulation, decreased function in terms of self-concept and judgment,

and an inability to maintain social interactions (Frederiksen & Waldemar, 2017; Psychogeriatric Interest Group of Chinese Society of Psychiatry, 2017), while irritability refers to reduced control over temper and verbal or behavioral manifestations including flashes of rage, sudden mood changes, impatience, and being argumentative and easily irritated (Frederiksen & Waldemar, 2017). In terms of the overlap among these four symptoms, there are no explicit boundaries defining the four concepts, and some psychiatrists have suggested combining these four factors into one in subsequent studies (Aalten *et al.*, 2003; Frederiksen & Waldemar, 2017). Therefore, it is necessary to study these disruptive behaviors as a cluster of symptoms instead of studying them as separate and unrelated behaviors.

Advanced structural magnetic resonance imaging (MRI) has been used to measure various morphological features such as cortical thickness, surface area, gray matter volume, and gyrification index. Cortical thickness and surface area measures can be used

to determine the thickness and area of the cortex rather than a comparatively meaningless voxel, as determined with voxel-based morphometry (Lerch et al., 2005). More specifically, the two measures have clearer physical meanings compared to other morphological measures: cortical thickness is associated with the number, size, and arrangement of cells within a column, while surface area is related to the number of columns within a certain cortical region (Xie et al., 2019). Thus, cortical thickness and surface area are appropriate and effective for investigating the neural mechanisms underlying behavioral problems.

Most previous studies about morphological features of AD have mainly focused on cognitive functions (Lerch et al., 2005). Cortical traits associated with emotional disorders in AD patients, such as depression and psychosis, have also been investigated in recent years (Lee et al., 2022; Zahodne et al., 2013). Using these measures, several prior studies have explored the relationship between cortical thickness and the severity of a single disruptive behavior in AD patients. For example, Trezpacz and colleagues found that agitation and aggression in patients with AD and with mild cognitive impairment are associated with reduced cortical thickness in the frontal and cingulate regions (Trzepacz et al., 2013). There are also documentations focusing on the relationship between other brain measurements and the multi-dimensional classification of disruptive behaviors in neurodegenerative disease patients (Cajanus et al., 2019). However, there is a paucity of studies examining the relationship between cortical thickness and multi-dimensional disruptive behaviors in AD. Thus, it is necessary to elucidate the neuroanatomical signatures, particularly the cortical thickness and surface area, of the brain that are related to disruptive behaviors in AD patients.

To fill the gap, the aim of this study was to investigate morphological characteristics of the brain associated with disruptive behaviors in patients with AD. We hypothesized that the neural substrates underlying disruptive behaviors are regions associated with emotional regulation and sensory perception.

Methods
Study participants

One hundred seventy-four participants (125 AD patients and 49 healthy controls) were selected from the clinical AD imaging database at Peking University Sixth Hospital. The clinical diagnosis of AD was made according to the ICD-10 and NINCDS-ADRDA diagnostic criteria (as previously described) (Wang et al., 2015). Patients were excluded if they had any of the following conditions: (i) structural abnormalities associated with other types of dementia; and (ii) other illnesses that affected cognitive function. The healthy controls had no history of neurological or psychiatric disorders, sensorimotor impairment, or cognitive issues; no abnormal anatomical findings in conventional brain MRIs; and no evidence of cognitive deficits in neuropsychological tests. MRI examinations were performed on all participants. The project was approved by the Institutional Review Board of Peking University Sixth Hospital. Written consent was provided for each participant.

Cognitive assessment and behavior evaluation

All participants were given comprehensive neuropsychology tests on global cognitive function and specific cognitive domains. In this study, the Mini-Mental State Examination (MMSE) (Folstein et al., 1975; Li et al., 1988; Shen et al., 2014), the Montreal Cognitive Assessment (MoCA) (Nasreddine et al., 2005), and the Cognitive Abil-

ities Screening Instrument (CASI) (Lin et al., 2012; Teng et al., 1994) were used to evaluate global cognitive status.

The Neuropsychiatry Inventory (NPI) (Cummings, 1997; Zhang et al., 2012) was used for behavioral evaluation. The sum of the agitation/aggression, disinhibition, irritability/lability, and aberrant motor activity subdomain scores was used to determine the severity of the disruptive behaviors.

MRI data acquisition

All subjects were scanned with a 3-Tesla magnetic resonance system with a Siemens Magnetom Trio. We acquired high-resolution three-dimensional T1-weighted anatomical images with a magnetization-prepared rapidly acquired gradient-echo sequence. The scans with the Siemens system had the following imaging parameters: repetition time (TR) = 2530 ms, echo time (TE) = 3.44 ms; time inversion (TI) = 1100 ms; slice thickness = 1.0 mm; no gap; slice number = 192; and matrix size = 256×256.

Image data processing

To calculate the cortical thickness and surface area, all images were processed using the CIVET pipeline [v.1.1.9. (Ad-Dab'bagh et al., 2006, Zijdenbos et al., 2002)]. Briefly, the original magnetic resonance images were first mapped to stereotaxic space using a linear transformation (Collins et al., 1994), and the nonuniformity of the induced magnetic fields was corrected using the N3 algorithm (Sled et al., 1998). A back-propagation artificial neural network classifier was used to segment each image into white matter, gray matter, cerebrospinal fluid, and noncerebral tissue (Zijdenbos et al., 2002). Then, the constrained Laplacian-based anatomic segmentation method and a proximity algorithm (Kim et al., 2005; MacDonald et al., 2000) were used to extract the inner and outer gray matter surfaces, with 81 924 vertices (40 962 on each hemisphere) identified.

The cortical thickness and surface area data were then obtained based on the extracted inner and outer gray matter surfaces. The vertex-wise cortical thickness was measured based on the linked distance between corresponding vertices on the two surfaces, which has been shown to be the simplest and most precise method for measuring cortical thickness (Lerch & Evans, 2005). The sensitivity was improved by smoothing with a 20-mm kernel (Chung et al., 2003). The surface area was evaluated on a mid-surface, i.e. a polyhedral mesh located directly between the inner and outer gray matter surfaces. The surface area of each vertex was defined as one-third of the total area of all triangles adjoining it and smoothed with a 20-mm kernel. The vertex-based statistical results were displayed on the T1 template of ICBM152 in the Montreal Neurological Institute space with the BrainNet Viewer toolbox (Xia et al., 2013).

While vertex-based analyses are sensitive to small cortical changes, region(s)-of-interest (ROI)-based analyses are resilient to spatial noise by obtaining mean cortical thickness or total surface area values within a given ROI. Therefore, after the cortical thickness and surface area of each vertex were calculated, the mean cortical thickness and total surface area of 78 cortical ROI were determined. The ROI were selected from the 90 ROI defined in the automated anatomical labeling (AAL) atlas (Gong et al., 2009; Tzourio-Mazoyer et al., 2002), with 12 excluded because they were not on the cortex (see Supplementary Text). The mean cortical thickness of each ROI was defined as the mean value of the cortical thickness of all vertices within the region, and the total surface area of each ROI was calculated by summing the surface areas of all vertices belonging within the region.

Table 1: The demographics, cognitive function, and disruptive behavioral features of the two groups.

	AD patient ($n = 125$)	Normal control ($n = 49$)	t/χ^2-value	P value
Age (years)	71.55 ± 7.1	69.0 ± 9.1	1.960	0.052
Gender (M/F)	30/95	20/29	3.699	0.054
Education (years)	11.3 ± 4.6	13.7 ± 3.3	− 3.296	0.001
MMSE	18.8 ± 4.2	28.5 ± 1.4	− 15.935	<0.001
MoCA	13.3 ± 4.6	25.9 ± 2.5	− 18.049	<0.001
CASI	69.0 ± 14.9	95.2 ± 3.5	− 12.184	<0.001
NPI				
Agitation/aggression	2.1 ± 3.2	0.2 ± 1.1	4.009	<0.001
Disinhibition	0.5 ± 1.6	0	2.168	0.032
Irritability/lability	2.2 ± 2.8	0.4 ± 1.4	4.262	<0.001
Aberrant motor behaviors	1.6 ± 3.3	0	3.480	0.001
Total score of disruptive behaviors	6.4 ± 8.1	0.5 ± 1.8	5.001	<0.001

Statistical analysis

A two-sample *t*-test was used to compare the age, years of education, MMSE score, MoCA score, CASI score, NPI agitation/aggression, disinhibition, irritability/lability, and aberrant motor activity subscores, and the total score of disruptive behaviors between AD patients and healthy controls. Sex was treated as a categorical variable and compared between the two groups with a chi-square test. Statistical significance was set at a P value < 0.05 when comparing demographics, cognitive function, and disruptive behavioral features of AD patients and healthy controls.

ROI-wise cortical thickness and surface areas of AD patients and healthy controls were analyzed and compared using a general linear model (GLM), with age, sex, and years of education as covariates. The P values were corrected for multiple comparisons using the slightly conservative Bonferroni correction to reduce type I error (Mumford, 2012). Statistical significance was set at a corrected P < 0.05. Vertex-wise cortical thickness and surface areas of AD patients and healthy controls were also analyzed and compared using a GLM, with age, sex, and years of education as covariates. Because of the multitude of vertices, the multiple comparisons would be too stringent if the Bonferroni correction was used, and type II errors would therefore not be well controlled. Thus, for vertex-based analysis, false discovery rate (FDR) correction was used to correct for the P values. The *q* value threshold was set at 0.05.

For the association analysis between cortical thickness and total scores of disruptive behaviors in patients with AD, ROI in which cortical thickness showed significant between-group differences were selected. ROI-wise cortical thickness was analyzed and regressed for the total score of disruptive behavior. GLM analysis was conducted, with age, sex, and years of education as covariates. The P values were corrected using FDR correction. The *q* value threshold was set at 0.05. Regression between surface area and total scores of disruptive behaviors was performed similarly.

Results

Demographics, cognitive function, and disruptive behavioral features

As shown in Table 1, there were no significant differences in age or sex between AD patients and healthy controls. AD patients had lower education levels than healthy controls (t = −3.296, P = 0.001). In comparison to healthy controls, AD patients had worse global cognitive status as shown from MMSE scores (t = −15.935, P < 0.001), MoCA scores (t = −18.049, P < 0.001), and CASI

scores (t = −12.184, P < 0.001). AD patients also had higher scores on disruptive behaviors (t = 5.001, P < 0.001) and the subdomain items of agitation/aggression (t = 4.009, P < 0.001), disinhibition (t = 2.168, P = 0.032), irritability/lability (t = 4.262, P < 0.001), and aberrant motor behaviors (t = 3.480, P = 0.001).

Comparison of cortical thickness between AD patients and controls

The ROI-based analysis showed a global thinning pattern in the AD patients as compared to normal controls. The cortical thinning was most prominent in the superior, inferior, and middle temporal gyri, superior and middle occipital gyri, Heschl gyrus, angular gyrus, inferior parietal gyrus, and cuneus (Table 2, Fig. 1A). Vertex-based cortical thickness analysis exhibited a similar thinning pattern as done by ROI-based thickness analysis (Fig. 1B).

Comparison of surface area between AD patients and controls

The ROI-based analysis revealed that compared with normal controls, patients with AD showed smaller surface areas in the left fusiform and left inferior temporal gyrus (Table 3, Fig. 2). Vertex-based analysis showed similar results while also additionally revealing smaller inferior occipital surface area and greater surface areas in the precuneus and parahippocampal and lingual gyri in AD patients.

Association between disruptive behaviors and cortical thickness and surface area

The brain-behavior association analyses showed a negative correlation between total scores of disruptive behaviors and cortical thickness values in the bilateral angular and superior temporal gyri, right inferior parietal gyrus, right calcarine, right superior and inferior occipital gyri, right Heschl gyrus, right supramarginal gyrus, left middle temporal gyrus, and left middle occipital gyrus (Table 4, Fig. 3). The regression of the ROI total surface areas did not show any significant results.

Discussion

In the present study, we found that AD patients had significant cortical thinning throughout the brain, mainly involving the medial and lateral temporal and parietal cortex, and smaller surface areas in the left fusiform and left inferior temporal gyrus. Importantly, we found that high total scores of disruptive behaviors were associated with cortical thinning in several regions related

Table 2: Summary of the *t* values, uncorrected *P* values, and corrected *P* values of the differences in the ROI-based mean cortical thickness between AD patients and normal controls.

ROI	t value	uncorrected P value	Bonferroni-corrected P value	FDR-corrected P value
Temporal_Sup_R	−5.467	1.62E-07*	<0.001	<0.001
Temporal_Inf_L	−5.441	1.84E-07*	<0.001	<0.001
Occipital_Sup_R	−5.409	2.13E-07*	<0.001	<0.001
Heschl_R	−5.332	3.08E-07*	<0.001	<0.001
Temporal_Inf_R	−5.326	3.17E-07*	<0.001	<0.001
Temporal_Pole_Sup_R	−5.206	5.55E-07*	<0.001	<0.001
Angular_R	−5.057	1.10E-06*	<0.001	<0.001
Temporal_Pole_Sup_L	−5.018	1.31E-06*	<0.001	<0.001
Parietal_Inf_R	−4.847	2.83E-06*	<0.001	<0.001
Temporal_Mid_R	−4.814	3.27E-06*	<0.001	<0.001
Occipital_Mid_L	−4.777	3.84E-06*	<0.001	<0.001
Cuneus_R	−4.706	5.22E-06*	<0.001	<0.001
Occipital_Mid_R	−4.658	6.44E-06*	<0.001	<0.001
Lingual_R	−4.623	7.47E-06*	<0.001	<0.001
Fusiform_R	−4.621	7.53E-06*	<0.001	<0.001
SupraMarginal_R	−4.500	1.26E-05*	<0.001	<0.001
Frontal_Sup_Medial_R	−4.399	1.92E-05*	0.001	<0.001
Supp_Motor_Area_R	−4.375	2.12E-05*	0.002	<0.001
Calcarine_R	−4.365	2.20E-05*	0.002	<0.001
Cingulum_Post_R	−4.362	2.23E-05*	0.002	<0.001
Occipital_Inf_R	−4.343	2.42E-05*	0.002	<0.001
Temporal_Sup_L	−4.299	2.89E-05*	0.002	<0.001
Parietal_Sup_R	−4.291	2.99E-05*	0.002	<0.001
Temporal_Mid_L	−4.201	4.29E-05*	0.003	<0.001
Supp_Motor_Area_L	−4.185	4.57E-05*	0.004	<0.001
Precuneus_R	−4.173	4.80E-05*	0.004	<0.001
Frontal_Mid_R	−4.080	6.92E-05*	0.005	<0.001
Angular_L	−4.057	7.59E-05*	0.006	<0.001
Occipital_Inf_L	−3.906	1.35E-04*	0.011	<0.001
Frontal_Sup_R	−3.772	2.24E-04*	0.017	<0.001
Frontal_Sup_Medial_L	−3.591	4.32E-04*	0.034	0.001
Precentral_R	−3.533	5.31E-04*	0.041	0.001
Rolandic_Oper_R	−3.491	6.14E-04*	0.048	0.001
Temporal_Pole_Mid_R	−3.491	6.15E-04*	0.048	0.001

*Shows statistical significance, i.e. the uncorrected *P* value is no greater than the uncorrected *P* value threshold calculated by Bonferroni correction (6.41E-04). ROI, region of interest; Sup, superior; Inf, inferior; Mid, middle; Post, posterior; Supp, supplemental; Oper, Opera.
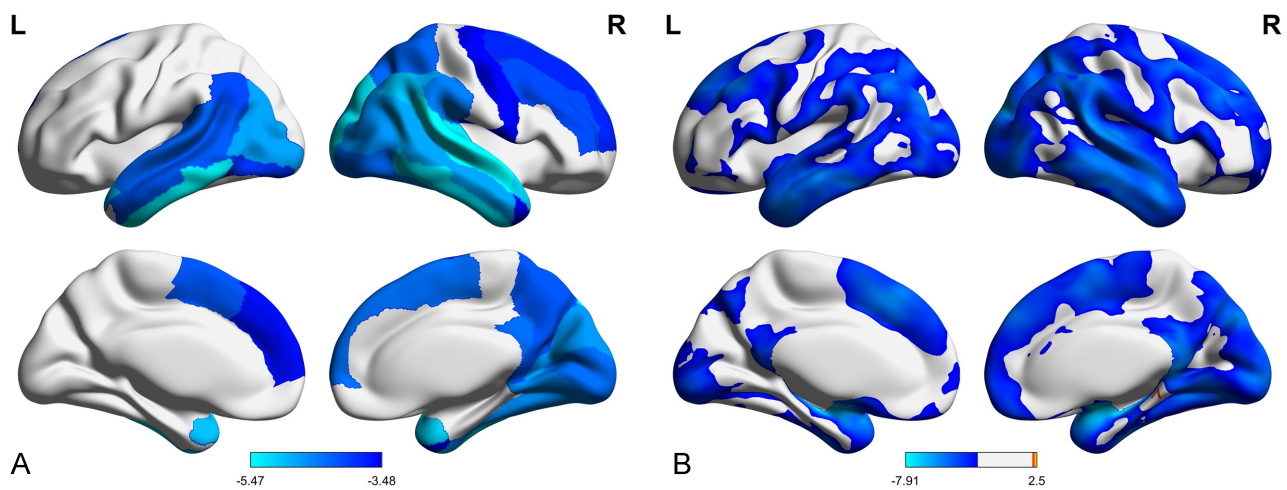

Figure 1: The *t*-statistic maps for comparison of cortical thickness between AD patients and healthy controls. (A) The *t*-statistic map for comparison of ROI-based cortical thickness between AD patients and healthy controls. Cold colors represent a thinner cortex in AD patients than in healthy controls. Lighter colors in the colored regions indicate a greater difference between the cortical thicknesses of the two groups. The uncorrected *t* value threshold obtained through Bonferroni correction is ±3.48. (B) The *t*-statistic map for comparison of vertex-based cortical thickness between AD patients and healthy controls. Cold colors represent a thinner cortex in AD patients than in healthy controls, while warm colors represent a thicker cortex in AD patients than in healthy controls. Lighter colors in the colored regions indicate a greater difference between the cortical thicknesses of the two groups. The uncorrected *t* value threshold obtained through FDR correction is ±2.18.

Table 3: Summary of the *t* values, uncorrected *P* values, and corrected *P* values of the differences in the ROI-based total surface areas between AD patients and normal controls.

ROI	t value	Uncorrected P value	Bonferroni-corrected P value	FDR-corrected P value
Fusiform_L	−3.727	2.64E-04*	0.021	0.020
Temporal_inferior_L	−3.529	5.37E-04*	0.042	0.020

*Shows statistical significance, i.e. the uncorrected *P* value is no greater than the uncorrected *P* value threshold calculated by Bonferroni correction (6.41E-04).
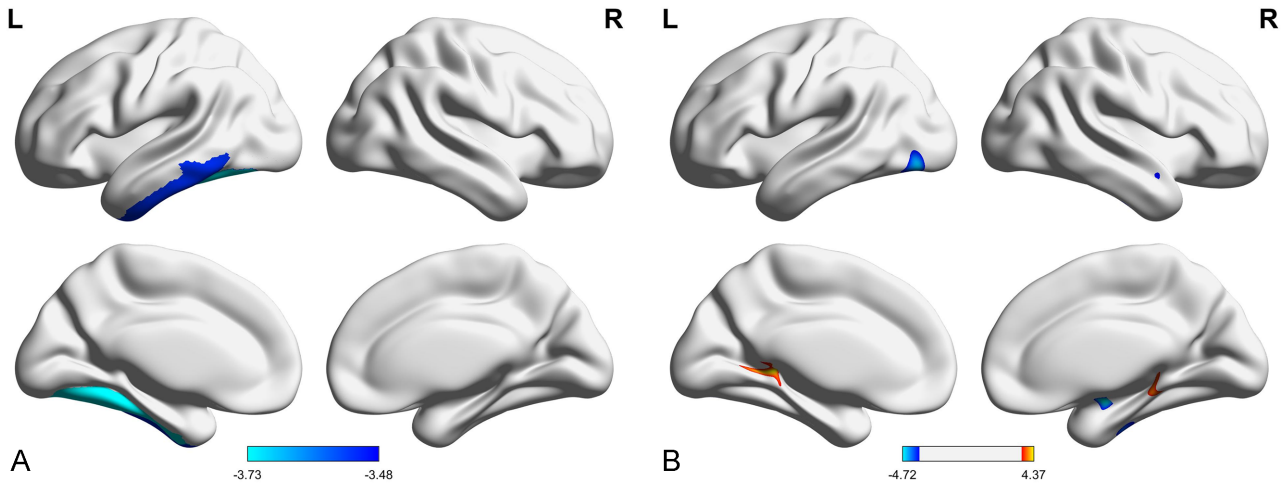

Figure 2: The *t*-statistic maps for comparison of surface area between AD patients and healthy controls. (A) The *t*-statistic map for comparison of ROI-based surface area between AD patients and healthy controls. Cold colors represent a smaller surface area in AD patients than in healthy controls, while warm colors represent a greater surface area in AD patients than in healthy controls. Lighter colors in the colored regions indicate a greater difference between the surface areas of the two groups. The uncorrected *t* value threshold obtained through Bonferroni correction is ±3.48. (B) The *t*-statistic map for comparison of vertex-based surface area between AD patients and healthy controls. Cold colors represent a smaller surface area in AD patients than in healthy controls, while warm colors represent a greater surface area in AD patients than in healthy controls. Lighter colors in the colored regions indicate a greater difference between the surface areas of the two groups. The uncorrected *t* value threshold obtained through FDR correction is ±3.54.

to sensorimotor processing, language, and expression functions. These results have important implications in understanding the neuroanatomical basis underlying disruptive behaviors in AD.

In this study, AD patients exhibited a widespread reduction of cortical thickness in the temporal, parietal, and occipital regions and a small reduction of cortical surface area in the left fusiform and left inferior temporal gyrus. Our findings were consistent with previous studies that compared cortical thickness in AD patients and healthy older adults (Julkunen *et al.*, 2010; Lerch *et al.*, 2005; Singh *et al.*, 2006). We also validated our results in the subgroup analysis in which the AD patients were divided into two subgroups according to the subjects' age rankings with a balanced sample size among groups (see Supplemental Table S1). Our findings were also consistent with results obtained using different biomarkers, including gray matter volume, white matter volume, and glucose metabolism (Busatto *et al.*, 2003; Jagust *et al.*, 2006; Matsuda, 2016).

Cortical thinning was observed in the superior and inferior parietal gyri and the middle temporal gyrus in people with more severe disruptive behaviors. Our findings are consistent with previously reported associations between disruptive behaviors and brain regions such as the parietal lobule (Yoshida *et al.*, 2015). The superior and inferior parietal gyri, and middle temporal gyrus are all located in the extrapyramidal motor cortex, which works with the primary motor cortex to control motor activity (Augustine, 2008). de Gois Vasconcelos *et al.* suggested that the parietal regions are responsible for executive dysfunction in AD patients (de Gois Vasconcelos *et al.*, 2014). Previous studies have linked the middle temporal gyrus to visual motor functions

(Felleman & Van Essen, 1987; Newsome & Pare, 1988). Our results suggest that cortical changes in motor-regulating areas could explain behavioral regulation issues during disruptive behaviors.

A previous study reported that inferior parietal activity was positively correlated with pleasant facial expressions shown to AD patients (Lee *et al.*, 2013). Another study found that the inferior parietal gyrus was involved in empathy for pain (Lamm *et al.*, 2011). We speculate that cortical changes in emotion-regulating regions may result in inappropriate sensory signal processing and, as a result, inappropriate responses to external stimuli.

Disruptive behaviors are also found to be closely related to sensory systems. In addition to being related to the motor cortex, the superior and inferior parietal gyri are important components of the dorsal "where" stream and ventral "what" stream for tactile object localization (Augustine, 2008). Mentis *et al.* suggested that the superior temporal and inferior parietal gyri are responsible for sensory association and that hypermetabolism in these gyri is related to delusional misidentification syndrome (DMS) (Mentis *et al.*, 1995). In our study, the severity of disruptive behaviors was found to be negatively correlated with cortical thickness in the superior, inferior, and middle occipital gyri, calcarine, superior and middle temporal gyri, and Heschl's gyrus (also known as the transverse temporal gyrus). The superior, inferior, and middle occipital gyri and calcarine are all located in the occipital lobe, which is believed to be responsible for vision awareness and visual information processing (Augustine, 2008). The superior temporal gyrus and Heschl's gyrus are both located in the primary auditory cortex, and the superior and middle temporal gyri are the main

Table 4: Summary of the *t* values, uncorrected *P* values, and corrected *P* values of the association between total scores of disruptive behaviors and the ROI-based mean cortical thickness.

ROI	t value	Uncorrected P value	FDR-corrected P value
Parietal_Inf_R	−3.161	0.002	0.039
Angular_L	−3.050	0.003	0.039
Calcarine_R	−2.919	0.004	0.039
Temporal_Sup_L	−2.862	0.005	0.039
Occipital_Sup_R	−2.814	0.006	0.039
Occipital_Inf_R	−2.634	0.010	0.049
Temporal_Mid_L	−2.571	0.011	0.049
Heschl_R	−2.513	0.013	0.049
Angular_R	−2.490	0.014	0.049
Occipital_Mid_L	−2.470	0.015	0.049
Temporal_Sup_R	−2.428	0.017	0.049
SupraMarginal_R	−2.416	0.017	0.049
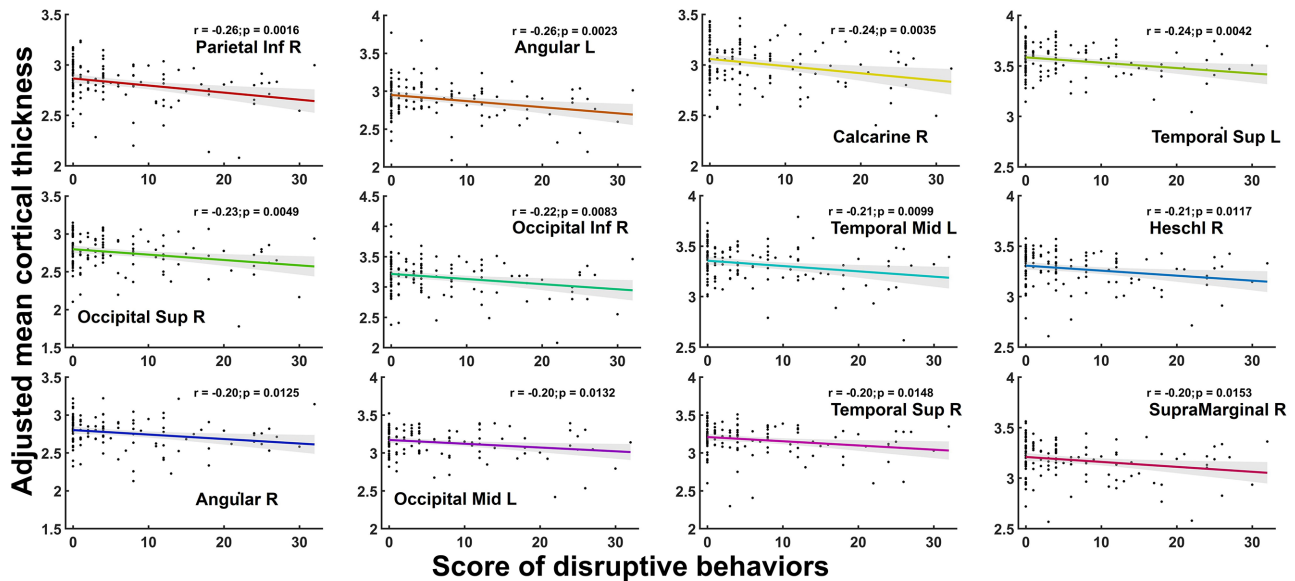
Figure 3: Scatterplots between the adjusted mean cortical thickness of selected ROI and the total score of disruptive behaviors. ROI that showed significant associations with the total score of disruptive behaviors were selected. The mean cortical thickness plotted was adjusted by subtracting covariate-caused influences. The black dots represent observed data points. The colored lines represent the regression line, while the light-gray region around each line represents the 95% confidence interval of the regression line.

components of the dorsal "where" stream in the auditory system (Augustine, 2008). Previous studies have reported that the superior temporal gyrus was active during auditory-related tasks such as name identification and auditory object segregation, and that it was thinner in people with logopenic progressive aphasia (lv-PPA) (Foxe *et al.*, 2016; Golden *et al.*, 2015). The middle temporal gyrus and Heschl's gyrus have been linked to abnormal auditory feedback processing during speech production and hearing loss, respectively (Ranasinghe *et al.*, 2019; Zainul Abidin *et al.*, 2021). In summary, our findings provide direct evidence that disruptive behaviors are closely related to the somatosensory, visual, and auditory systems.

Besides, we observed that disruptive behaviors were associated with cortical thinning in the supramarginal and angular gyri. This could imply that disruptive behaviors are related to language and expression functions. The supramarginal and angular gyri are both involved in language function. Injuries to the supramarginal gyrus, angular gyrus, and opercular part of the inferior frontal gyrus result in conductive, visual receptive, and expressive/motor aphasia, respectively (Augustine, 2008). The supra-

marginal and angular gyri have also been linked to autism spectrum disorder, which causes deficits in social communication (Zürcher *et al.*, 2021). In patients with AD, hypoperfusion of the supramarginal and angular gyri were associated with the scores of the Alzheimer's disease assessment scale-cognitive subscale, which has "language" as one of its subgroups (Shirayama *et al.*, 2019). Other studies have reported that inferior frontal thickness is negatively correlated with letter and category fluency in verbal fluency tasks and that fluorodeoxyglucose-positron emission tomography hypometabolism of the inferior frontal gyrus can distinguish the behavioral variant of frontotemporal dementia from the behavioral/dysexecutive variant of AD (Bergeron *et al.*, 2020; Vonk *et al.*, 2019). Our findings indicate that changes in the cortices that control language and expression may lead to an inability to fully comprehend others' words or an inability to respond appropriately to external stimuli, thus resulting in aberrant behaviors.

Several issues need to be further considered. First, although our study revealed an association between disruptive behaviors and certain brain structural changes, the causality between disruptive behaviors and brain structure was not clearly established. In

future studies, the use of *in situ* environmental monitoring technology and longitudinal design is important to aid in examining the temporal relationship between external stimuli and disruptive behaviors. The findings of this study are expected to elucidate the potential causality between disruptive behaviors and changes in brain structure. Second, our study relied solely on structural data, which could be biased because functional activity was not integrated. In subsequent studies, cortical thickness, surface area, and functional MRI data could be integrated to depict a more comprehensive profile of the neural substrates associated with the occurrence of disruptive behaviors. Finally, this study employed a widely used AAL template to parcellate the whole cerebral cortex into different ROI. Currently, there is a third version, AAL3 (Rolls *et al.*, 2020), which adds some regions not previously defined. Notably, these new regions included in the AAL3 are involved in the subdivisions of anterior cingulate cortex and thalamus that are not associated with the core results of our study. Thus, our conclusions are not affected by different versions of AAL atlases.

Conclusion

Disruptive behaviors in AD patients are most likely associated with cortical thinning in sensory, motor, and language regions. The findings of this study reflect the clinical hypothesis that aggravated cognitive impairment, motor and emotional control abnormalities, sensory dysfunction, and ineffective verbal communication might precipitate agitation, aggression, and disturbing behaviors. Further investigations are needed to deepen our understanding of the role of brain structural and functional abnormalities in disruptive behaviors.

Supplementary Data

Supplementary data are available at *Psychoradiology* online.

Author Contributions

R.X.: conceptualization, study design, imaging data computation, data analysis and interpretation, writing of the original draft preparation, and revising. T.X., H.Z., T.L., G.G., X.Y.: data curation, supervision of data analysis, writing, reviewing, and editing. Y.H.: supervision, study design, methodology, data interpretation, writing, reviewing, and editing.

Conflict of Interest

All authors report no financial interests or potential conflicts of interest. One of the authors, Y.H., is also the editorial-board member of *Psychoradiology*. He was blinded from reviewing or making decisions on the manuscript.

Acknowledgement

References

Aalten P, de Vugt ME, Lousberg R, *et al.* (2003) Behavioral problems in dementia: a factor analysis of the Neuropsychiatric Inventory. *Dement Geriatr Cogn Disord* **15**:99–105.

Ad-Dab'bagh Y, Einarson D, Lyttelton O, *et al.* (2006) The CIVET image-processing environment: a fully automated comprehensive pipeline for anatomical neuroimaging research. In: Corbetta M, Nichols T, Pietrini P (eds.), *Proceedings of the 12th Annual Meeting of the Organization for Human Brain Mapping*. Neuroimage.

Alzheimer's Disease International. (2015) *World Alzheimer Report 2015: the global impact of dementia: an analysis of prevalence, incidence, cost and trends*. https://www.alzint.org/resource/world-alzheimer-report-2015/.

Alzheimer's Disease International. (2021) *World Alzheimer Report 2021: journey through the diagnosis of dementia*. https://www.alzint.org/resource/world-alzheimer-report-2021/.

Augustine JR (2008) *Human Neuroanatomy* 1st edn. Elsevier.

Bergeron D, Sellami L, Poulin S, *et al.* (2020) The behavioral/dysexecutive variant of Alzheimer's disease: a case series with clinical, neuropsychological, and FDG-PET characterization. *Dement Geriatr Cogn Disord* **49**:518–25.

Busatto GF, Garrido GEJ, Almeida OP, *et al.* (2003) A voxel-based morphometry study of temporal lobe gray matter reductions in Alzheimer's disease. *Neurobiol Aging* **24**:221–31.

Cajanus A, Solje E, Koikkalainen J, *et al.* (2019) The association between distinct frontal brain volumes and behavioral symptoms in mild cognitive impairment, Alzheimer's disease, and frontotemporal dementia. *Front Neurol* **10**:1059.

Chung MK, Worsley KJ, Robbins S, *et al.* (2003) Deformation-based surface morphometry applied to gray matter deformation. *Neuroimage* **18**:198–213.

Collins DL, Neelin P, Peters TM, *et al.* (1994) Automatic 3D intersubject registration of MR volumetric data in standardized Talairach space. *J Comput Assist Tomogr* **18**:192–205.

Cummings JL (1997) The Neuropsychiatric Inventory: assessing psychopathology in dementia patients. *Neurology* **48**:10S–6S.

de Gois Vasconcelos L, Jackowski AP, de Oliveira MO, *et al.* (2014) The thickness of posterior cortical areas is related to executive dysfunction in Alzheimer's disease. *Clinics* **69**:28–37.

Felleman DJ, Van Essen DC (1987) Receptive field properties of neurons in area V3 of macaque monkey extrastriate cortex. *J Neurophysiol* **57**:889–920.

Folstein MF, Folstein SE, McHugh PR (1975) "Mini-mental state." *J Psychiatr Res* **12**:189–98.

Foxe D, Leyton CE, Hodges JR, *et al.* (2016) The neural correlates of auditory and visuospatial span in logopenic progressive aphasia and Alzheimer's disease. *Cortex* **83**:39–50.

Frederiksen KS, Waldemar G (2017) Aggression, agitation, hyperactivity, and irritability. In: Verdelho A, Gonçalves-Pereira M (eds.), *Neuropsychiatric Symptoms of Cognitive Impairment and Dementia*. Springer International Publishing, 199–236. https://doi.org/10.1007/978-3-319-39138-0_9.

Golden HL, Agustus JL, Goll JC, *et al.* (2015) Functional neuroanatomy of auditory scene analysis in Alzheimer's disease. *NeuroImage: Clinical* **7**:699–708.

Gong G, He Y, Concha L, *et al.* (2009) Mapping anatomical connectivity patterns of human cerebral cortex using in vivo diffusion tensor imaging tractography. *Cereb Cortex* **19**:524–36.

Jagust W, Gitcho A, Sun F, *et al.* (2006) Brain imaging evidence of preclinical Alzheimer's disease in normal aging. *Ann Neurol* **59**:673–81.

Julkunen V, Niskanen E, Koikkalainen J, *et al.* (2010) Differences in cortical thickness in healthy controls, subjects with mild cognitive impairment, and Alzheimer's disease patients: a longitudinal study. *J Alzheimers Dis* **21**:1141–51.

Kim JS, Singh V, Lee JK, *et al.* (2005) Automated 3-D extraction and evaluation of the inner and outer cortical surfaces using a

Laplacian map and partial volume effect classification. *Neuroimage* **27**:210–21.

Lamm C, Decety J, Singer T (2011) Meta-analytic evidence for common and distinct neural networks associated with directly experienced pain and empathy for pain. *Neuroimage* **54**:2492–502.

Lee TMC, Sun D, Leung M-K, *et al.* (2013) Neural activities during affective processing in people with Alzheimer's disease. *Neurobiol Aging* **34**:706–15.

Lee Y-M, Park J-M, Lee B-D, *et al.* (2022) The role of decreased cortical thickness and volume of medial temporal lobe structures in predicting incident psychosis in patients with Alzheimer's disease: a prospective longitudinal MRI study. *Am J Geriatr Psychiatry* **30**:46–53.

Lerch JP, Evans AC (2005) Cortical thickness analysis examined through power analysis and a population simulation. *Neuroimage* **24**:163–73.

Lerch JP, Pruessner JC, Zijdenbos A, *et al.* (2005) Focal decline of cortical thickness in Alzheimer's disease identified by computational neuroanatomy. *Cereb Cortex* **15**:995–1001.

Li G, Shen Y, Chen C, *et al.* (1988) [Study on the brief testing for dementia: testing MMSE among urban elderly]. *Chinese Ment Health J* **2**:13–8.

Lin K-N, Wang P-N, Liu H-C, *et al.* (2012) [Cognitive Abilities Screening Instrument, Chinese Version 2.0 (CASI C-2.0): administration and clinical application]. *Acta Neurol Taiwan* **21**:180–9.

MacDonald D, Kabani N, Avis D, *et al.* (2000) Automated 3-D extraction of inner and outer surfaces of cerebral cortex from MRI. *Neuroimage* **12**:340–56.

Matsuda H (2016) MRI morphometry in Alzheimer's disease. *Ageing Res Rev* **30**:17–24.

Mentis MJ, Weinstein EA, Horwitz B, *et al.* (1995) Abnormal brain glucose metabolism in the delusional misidentification syndromes: a positron emission tomography study in Alzheimer disease. *Biol Psychiatry* **38**:438–49.

Mumford JA (2012) A power calculation guide for fMRI studies. *Soc Cogn Affect Neurosci* **7**:738–42.

Nasreddine ZS, Phillips NA, Bédirian V, *et al.* (2005) The Montreal Cognitive Assessment, MoCA: a brief screening tool for mild cognitive impairment. *J Am Geriatr Soc* **53**:695–9.

Newsome W, Pare E (1988) A selective impairment of motion perception following lesions of the middle temporal visual area (MT). *J Neurosci* **8**:2201–11.

Psychogeriatric Interest Group of Chinese Society of Psychiatry. (2017) Expert consensus on the clinical management of neuropsychiatric syndromes in neurocognitive disorders. *Chinese J Psych* **50**:335–9.

Ranasinghe KG, Kothare H, Kort N, *et al.* (2019) Neural correlates of abnormal auditory feedback processing during speech production in Alzheimer's disease. *Sci Rep* **9**:5686.

Rolls ET, Huang C-C, Lin C-P, *et al.* (2020) Automated anatomical labelling atlas 3. *Neuroimage* **206**:116189.

Shen JH, Shen Q, Yu H, *et al.* (2014) Validation of an Alzheimer's disease assessment battery in Asian participants with mild to moderate Alzheimer's disease. *Am J Neurodegen Dis* **3**:158–69.

Shirayama Y, Takahashi M, Oda Y, *et al.* (2019) RCBF and cognitive impairment changes assessed by SPECT and ADAS-cog in late-onset Alzheimer's disease after 18 months of treatment with the cholinesterase inhibitors donepezil or galantamine. *Brain Imag Behav* **13**:75–86.

Singh V, Chertkow H, Lerch JP, *et al.* (2006) Spatial patterns of cortical thinning in mild cognitive impairment and Alzheimer's disease. *Brain* **129**:2885–93.

Sled JG, Zijdenbos AP, Evans AC (1998) A nonparametric method for automatic correction of intensity nonuniformity in MRI data. *IEEE Trans Med Imaging* **17**:87–97.

Teng EL, Hasegawa K, Homma A, *et al.* (1994) The Cognitive Abilities Screening Instrument (CASI): a practical test for cross-cultural epidemiological studies of dementia. *Int Psychogeriatr* **6**: 45–58.

Trzepacz PT, Yu P, Bhamidipati PK, Alzheimer's Disease Neuroimaging Initiative, *et al.* (2013) Frontolimbic atrophy is associated with agitation and aggression in mild cognitive impairment and Alzheimer's disease. *Alz Dement* **9**:S95–104.e1. https://doi.org/10.1016/j.jalz.2012.10.005.

Tzourio-Mazoyer N, Landeau B, Papathanassiou D, *et al.* (2002) Automated anatomical labeling of activations in SPM using a macroscopic anatomical parcellation of the MNI MRI single-subject brain. *Neuroimage* **15**:273–89.

Vonk JMJ, Rizvi B, Lao PJ, *et al.* (2019) Letter and category fluency performance correlates with distinct patterns of cortical thickness in older adults. *Cereb Cortex* **29**:2694–700.

Wang X, Wang J, He Y, *et al.* (2015) Apolipoprotein E ε4 modulates cognitive profiles, hippocampal volume, and resting-state functional connectivity in Alzheimer's disease. *J Alzheimers Dis* **45**: 781–95.

Xia M, Wang J, He Y (2013) BrainNet Viewer: a network visualization tool for human brain connectomics. *PLoS ONE* **8**:e68910.

Xie T, Zhang X, Tang X, *et al.* (2019) Mapping convergent and divergent cortical thinning patterns in patients with deficit and nondeficit schizophrenia. *Schizophr Bull* **45**:211–21.

Yoshida T, Mori T, Yamazaki K, *et al.* (2015) Relationship between regional cerebral blood flow and neuropsychiatric symptoms in dementia with Lewy bodies: neuropsychiatric symptoms and rCBF in DLB. *Int J Geriatr Psychiatry* **30**:1068–75.

Zahodne LB, Gongvatana A, Cohen RA, *et al.* (2013) Are apathy and depression independently associated with longitudinal trajectories of cortical atrophy in mild cognitive impairment? *Am J Geriatr Psychiatry* **21**:1098–106.

Zainul Abidin FN, Scelsi MA, Dawson SJ, *et al.* (2021) Glucose hypometabolism in the auditory pathway in age related hearing loss in the ADNI cohort. *NeuroImage: Clinical* **32**:102823.

Zhang M, Wang H, Li T, *et al.* (2012) Prevalence of neuropsychiatric symptoms across the declining memory continuum: an observational study in a memory clinic setting. *Dement Geriatr Cogn Disord Extra* **2**:200–8.

Zijdenbos AP, Forghani R, Evans AC (2002) Automatic "pipeline" analysis of 3-D MRI data for clinical trials: application to multiple sclerosis. *IEEE Trans Med Imaging* **21**:1280–91.

Zürcher NR, Loggia ML, Mullett JE, *et al.* (2021) [11C]PBR28 MR–PET imaging reveals lower regional brain expression of translocator protein (TSPO) in young adult males with autism spectrum disorder. *Mol Psychiatry* **26**:1659–69.